MULTI-PHYSICS SIMULATION OF CO_2 GAS COOLERS USING EQUIVALENCE MODELING

Antonio Rossetti, Sergio Marinetti, Silvia Minetto
National Research Council, Construction Technology Institute, Corso Stati Uniti,4
35127 Padova, Italy
antonio.rossetti@itc.cnr.it

ABSTRACT

A CFD model to simulate CO_2 gas coolers is presented: the adoption of an equivalent approach allows to reproduce the effects of an extended finned surface while drastically reducing the computational effort.
The model is validated against experimental results available in the open literature. The contemporary solution of both convection and conduction allows highlighting the impact of conduction along the tubes and the supporting end plates. The model provides satisfactory matching with experimental results: total heating power is forecast within 2.5%, while the maximum temperature deviation between the simulated and experimental heat exchanger curves temperature is 3.8 °C, when the CO_2 temperature is as high as 108 °C.
This thermal CFD model allows evaluating the 3D effects of the air maldistribution in terms of temperature, heat transfer coefficients, and cooling power, thus opening the way to the simulation and optimisation of complete ventilated finned coil and gas cooling systems.

Keyword: CFD; Multi-physics simulation; Heat-Exchanger; Fins and Tube; CO2; Transcritical

1 INTRODUCTION

Gas cooler design is crucial to maximise performances of CO_2 systems: the choice of the number of circuits and their arrangement heavily influences the overall performance. Because CO_2 thermophysical properties strongly vary during the heat rejection process, a distributed method, capable of solving the energy equation in terms of local equilibrium, is required to predict accurately the heat transfer coefficient.
The gas cooler modelling needs to properly account for to the wide variations of the thermodynamical and transport properties of the refrigerant near the critical point. Many methods are presented in the literature to rate or design heat exchangers (Sha and Sekulic, 2003), and, despite simplifying hypothesis, they normally provide very good results. However, when dealing with complex cases, like two-phase flow, air dehumidification or variable fluid properties, as it happens for transcritical carbon dioxide, a mesh is needed to obtain a division of the heat exchangers into cells together with a numerical scheme for equations discretisation and the solution of the resulting system of equations. A wide literature concerning the solution to the above-mentioned problems by discretisation techniques does exists.
Many authors have dealt with gas cooler models, able to account also for conduction from tube to tube.
In particular, Singh *et al.*, 2010 worked out a heat exchanger model which, besides considering conduction between tubes, is also able to simulate discontinuous fins. The technique of cutting fins to limit tube-to-tube conduction in gas coolers was previously identified by Zilio et al, 2007. Ge and Cropper, 2009, gave relevant contribution, providing a validated models which can be utilised for heat exchanger design and optimisation.

When the numerical modelling of heat exchangers is addressed, two distinct approaches can be distinguished: the use of correlation based concentrated models and the use of CFD codes, which solves fluid governing equation.
Concentrated parameters models can provide reliable and computationally fast solutions, allowing to critically discuss the main design parameters and optimal operating conditions (Gupta and Dasgupta, 2014), or to couple them with iterative optimization techniques (Mona *et al.* 2017). Correlation models (such as the ε-NTU method) are capable of handling to some extent the effects of air maldistribution (Bensafi *et al.*, 1997; Koern *et al*. 2011, Koern *et al*. 2013, Mao *et al*. 2013) upstream, inside and downstream the evaporator.
On the other side, these models are intrinsically limited by the minimum size of the periodic element and by the fact that they do not solve convection, requiring analytical correlations for convective heat transfer coefficients and the previous knowledge of the air profiles, which are usually unknown in real case applications.
In addition, CFD modelling offers the opportunity of fully accounting for heat conduction through fins, which is a more relevant problem in gas coolers rather than in condensers, due to the non-isothermal heat rejection and the large refrigerant temperature drop which causes non-negligible heat transfer from tube to tube via fin conductions, depending on circuit arrangement. This problem was properly highlighted and described in Zilio et al, 2007.
CFD has proved to be an effective tool to handle complex 3D flows (Aslam Bhutta *et al*., 2012). Due to the significant computational cost of reliable CFD analysis solving non isothermal fluid flow in presence of extended wetted surfaces, the great part of CFD applications in the heat exchanger design is limited to the discretization of just one fin passage under symmetry and periodic condition. These models can be successfully applied to investigate different aspects of the heat transfer processes, as the optimum tube shape and layout (Lanping Zhao *et al.* 2017); the effect of louvers and winglet geometry on the fluid flow (Shina *et al.*, 2016; Dezan *et al*. 2016); the impact of air velocity uneven profiles on the tube pitch scale (Wahiba *et al.* 2016) or the best material-efficient fin to obtain efficient and light geometries (Singh et al 2017). Santosa et al. (2017) proposed a CFD model of a gas cooler which, under some simplification assumptions, was able to provide insight in the local air and refrigerant side heat transfer coefficients and temperature distribution.
Although computationally long and expensive, some approaches to the full 3D simulation of the whole heat exchanger are reported in literature. For example Moukalled *et al.* (2011) used a 3D CFD code to model and optimise the air flow on a rooftop air conditioning unit. The model included all the main causes of air maldistribution such as the casing and the fans; heat transfer was solved modelling all the fins of both evaporator and condenser units.
Correlation based models and CFD present complementary advantages and limits. One of the main drawbacks of the former approach is the lack of flexibility in the description of complex 3D fields, while the latter relies on huge computational efforts, requiring long time and expensive hardware to get results.
For these reasons, other approaches have been proposed. Singh *et al.* (2011) suggested a combined method, were the flow field obtained by a CFD model allowed to provide the mass flow to algebraic discrete model of the heat exchanger.
Fluid dynamic equivalent resistance can be used to reduce the complexity of 3D CFD models, as demonstrated by Rossetti *et al.* (2015a) and Rossetti *et al.* (2015b). Marinetti *et al.* (2013) also proposed the use of PIV experimental data to avoid the inclusion of the fans into the model, preserving at the same time the information necessary to reproduce the experimental maldistribution of air impacting the evaporator in

the numerical model. Soo Lee et al. (2018) coupled the fluid dynamic equivalence resistance approach on a CFD model of the air side of an A-coil heat exchanger, with ε-NTU method solving for the energy balance.

In this paper, a 3D CFD model of a gas cooler is presented, adopting an equivalent approach which is design to reduce the computational load of the 3D CFD simulation. At the same time, the presented model maintains the most attractive features of CFD such as the independence from previous knowledge on the fin performances and the capability to handle complex and uneven air profiles. The present equivalence model is an improved formulation of the fluid (Rossetti *et al.* 2015a) and thermo-fluid (Rossetti *et al.* 2015b) models. The main advancement is the capability to account for both the conduction and convection phenomena taking place in the heat exchanger, solving the refrigerant, the solid and the air domains at the same time. The approximation of the finned volume to a properly homogenous porous medium, allows for significant reduction of the numerical complexity of the problem. The model is validated against experimental data available in the open literature (Zilio *et al.*, 2007, Schiochet, 2005).

The developed model will offer a tool to analyse gas coolers in operation, considering air maldistribution due to fan and plenum arrangements or fan modulation and switch off.

2 CASE STUDY

The model is developed starting from the finned coil geometry presented in Zilio *et al.* (2007) and Schiochet (2005), whose experimental data are used to validate the model itself. The considered gas cooler is a fin a tube heat exchanger, with a frontal area of 0.5 x 0.5m, 2 circuits and 4 rows. Fig. 1a shows the tube arrangement of the reference geometry, while in Fig. 1b and c the louvered aluminium fins geometry is presented. Table 1 summarizes the main dimensional characteristic of the fin and tube heat exchanger.

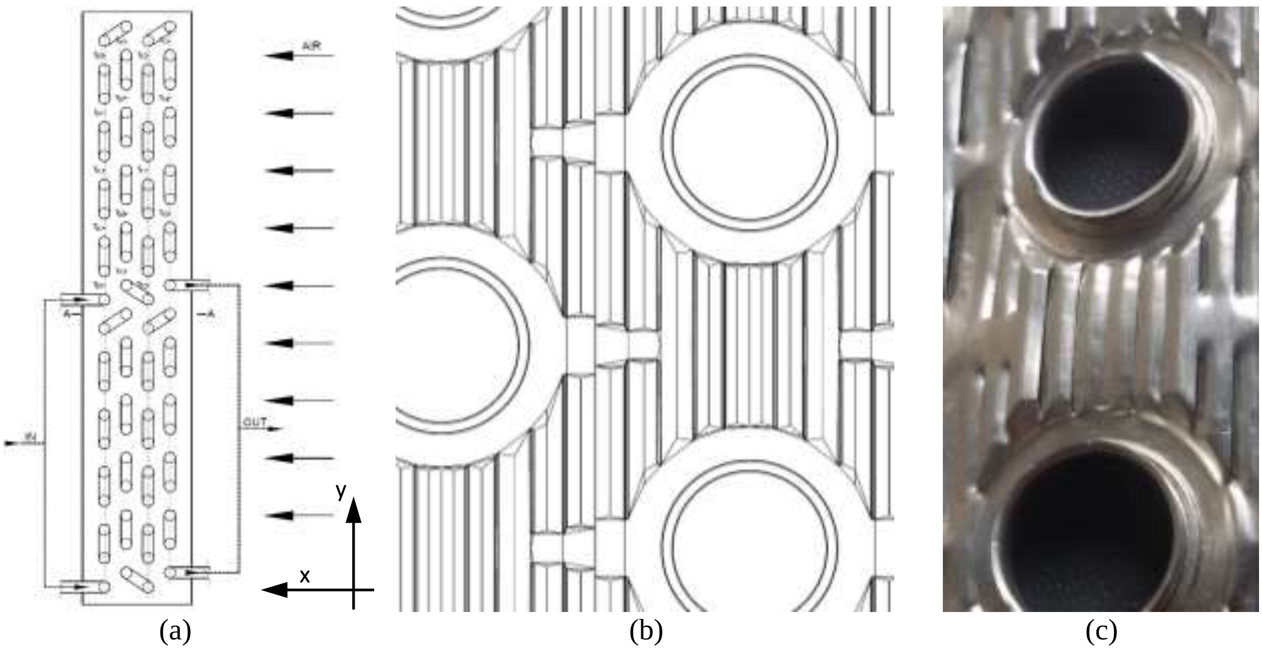

Fig. 1. Heat Exchanger geometry: (a) tube arrangement; (b) fin geometry; (c) fin detail.

Experimental data were collected on a dedicated test rig. The analysed gas cooler rejects the heat on the high pressure side of a a two stage intercooled compression CO_2 circuit; two separate closed loop air circuits dedicated to the gas cooler and the evaporator and three auxiliary water circuits used to feed the intercooler

and to recondition the air temperature in the two air circuits. The fine tuning of the air temperature is then achieved by mean of PID controlled electrical heaters. The complete description of the test facility, comprehensive of the measuring procedure and the uncertainty analysis are reported the original papers of Zilio *et al.* (2007) and Schiochet (2005).
A Cartesian reference system is adopted for all the models of the present paper, with the following convention: x-direction is aligned to the undisturbed velocity vector; y-direction is normal to the x direction and laying in the fin plane; z-direction normal to the fins plane.

Table 1. Geometrical and material characteristics of the heat exchanger

Feature	**Value**	**Unit**
Width x Height	500 x 500	10^{-3} m
Tube pitch	25	10^{-3} m
Row pitch	19	10^{-3} m
Fin pitch	2.1	10^{-3} m
Fin thickness	0.1	10^{-3} m
Tube external diameter	9.52	10^{-3} m
Tube thickness	0.65	10^{-3} m
Fin material	Al	
Tube material	Cu	
Side Plates material	Iron	

3 Numerical Model

3.1 The equivalence approach

The detailed numerical simulation of heat exchangers is a computationally expensive problem. In fact, the large extension of wetted area, i.e. contact area between the solid and air domain, forces the use of a large amount of nodes: the momentum and energy exchange between the fluid and the surface requires in fact fine grids to be correctly discretized and solved. Furthermore, when both the refrigerant and the air are considered on the fluid-dynamic point of view, conduction on the solid part of the heat exchanger needs to be accounted for in order to correctly couple the energy transfer between the two fluids.
The use an equivalent method can drastically simplify the discretization problem, as demonstrated in [Rossetti *et al*., 2015a and 2015b]. This approach assumes that a fin cascade can be approximated to a proper porous media when the fin pitch is negligible when compared to the other dimensions of the heat exchanger. In the equivalent porous media, fluid and solid coexist and interact by means of volumetric quantities instead of surface interaction. This operation can be interpreted as the application of a spatial low-pass filter to the model using the pitch as a threshold. While it entirely removes details smaller than the fin-pitch, it preserves the distributions on the larger scale. At the same time, it significantly decreases the minimum length scale used for the grid generation. On the other side, the interaction between the fluid and the fictional porous medium must be carefully set to correctly reproduce all the effects of the fin pack, preserving the model accuracy.

The equivalence model, on the solid side, should reproduce the fin conduction behaviour as well as the thermal capacity of the original louvered fin geometry. On the fluid side, all the main surface-to-fluid interactions had to be accounted and replicated.

The equivalence model was obtained by means of modification of the physics equations. The fitting of these models to the real geometry is discussed in the next session.

The solid volume fraction θ is defined as the fraction of the overall volume occupied by the solid. For a fin pack this ratio can be simplified to the ratio between the fin thickness and the fin pitch, resulting, for the current geometry, $\theta = 4.8\%$. The energy equation in the solid and the fluid domain should then be rearranged accordingly to the actual volume fraction:

$$(1-\theta)\rho Cp\, \mathbf{u}_a \cdot \nabla T_a - \nabla \cdot \left((1-\theta) k_a \nabla T_a\right) = Q \tag{1}$$

$$\nabla \cdot \left(-\theta \mathbf{k}_s \nabla T_s\right) = -Q \tag{2}$$

where Q is the heat flux between solid and fluid. The porous medium was considered to have anisotropic conduction coefficients $\mathbf{k}_s$, in order to simulate the fin behaviour. Equations 1 and 2 allow equating the thermal capacity and conductivity of the equivalence model to the actual one.

When considering the effect of the fins on the fluid momentum equation, three different aspects had to be addressed: the drag losses, the physical separation between two adjacent passages and the Reynolds number sudden reduction.

The drag was reproduced assuming a distributed anisotropic loss model, which is then added as volumetric force $\mathbf{F}_L$ to the heat exchanger domain:

$$\mathbf{F}_L = -\rho \mathbf{f}_L \cdot \frac{(\mathbf{u} \cdot \mathbf{u})}{2}\,\hat{\mathbf{t}} \tag{3}$$

where $\hat{\mathbf{t}}$ is the unit vector parallel to the flow velocity $\mathbf{u}$.

While eq. 3 can be used to prevent on the equivalent model the presence of velocity components along the fin normal direction, it is not sufficient to prevent the momentum exchange on this direction due to viscous forces. In order to avoid any momentum transfer through the fin plane, the stress tensor should then be modified inside the equivalent domain, removing the contribution of the gradients along the fin normal.

The turbulent to laminar transition inside the heat exchanger was induced using a scalar variable *i* (for intermittency), as fully explained by Menter *et al.* (2004). Intermittency is used as a multiplying factor to the turbulence kinetic energy source term, so that the model can be forced to switch between laminar behaviour (*i = 0)* and standard turbulent behaviour (*i = 1).* As the transition location is known and corresponds to the finned volume of the gas cooler, no equation is solved in order to obtain the transition: intermittency is prescribed as a function of the geometrical reference system, assuming a second order continuous blend of 20 mm between the heat exchanger volume (*i = 0*) and the external volume (*i = 1*).

The surface energy flux was reformulated by a volumetric source term based on the air local temperature, the equivalent solid temperature and a volumetric convective coefficient α expressed in $Wm^{-3}K^{-1}$. The form of the volumetric source in a volume *dV* is set to equate the heat flow of an elementary volume of area *dA,* with height equal to the fin pitch *b*:

$$\alpha_a\ 2dA\left(T_a - T_s\right) = \not\alpha_a\ dV\left(T_a - T_s\right) \tag{4}$$

where 2 accounts for the two sides of the fin enclosed in *dV*. As *dV = dA b*, the volumetric convective coefficient $\not\alpha$ can be expressed as a function of the surface convective coefficient α , then obtaining:

$$\not\alpha_a = 2\alpha_a / b \tag{5}$$

The following formulation for the heat exchange was then added to both the fluid energy equation (see eq.1):

$$Q = \not\alpha_a\left(T_s - T_a\right) \tag{6}$$

All the numerical models were developed using commercial software COMSOL Multiphysics 5.3.

3.2 Fin Simulation and tuning of the equivalence model

In order to set the equivalence model, a single fin simulation was carried out. The models take advantage from the symmetries and the periodicities of the fin geometry. The detailed and the simplified models are presented in Fig. 2, where the boundary surfaces are highlighted using different colours, according to the legend of Fig. 2.

Fluid flow was modelled as a laminar flow. The fin thickness was neglected in the detailed model to simplify the discretization, assuming that an ideal 2D surface is a reasonable approximation of the real geometry. Conduction through the fin was accounted for by applying conduction equation for thin shells.

Both simulations were set using the same 2D boundary conditions. Specifically, for the fluid flow, the conditions are: uniform velocity at inlet ($\mathbf{u} = 1.6$ m s^{-1}), relative static pressure at outlet (p = 0 Pa), no slip condition on the tubes and fin surfaces, symmetry on the tube cross section plane and periodicity on the orthogonal plane to reproduce an infinite fin cascade. As the thermal problem is concerned, boundary conditions include uniform temperature on the inflow ($T_a = 23$ °C) and constant temperature on the tube surfaces, extrapolated from the experimental data reported in Zilio *et al.* (2007).

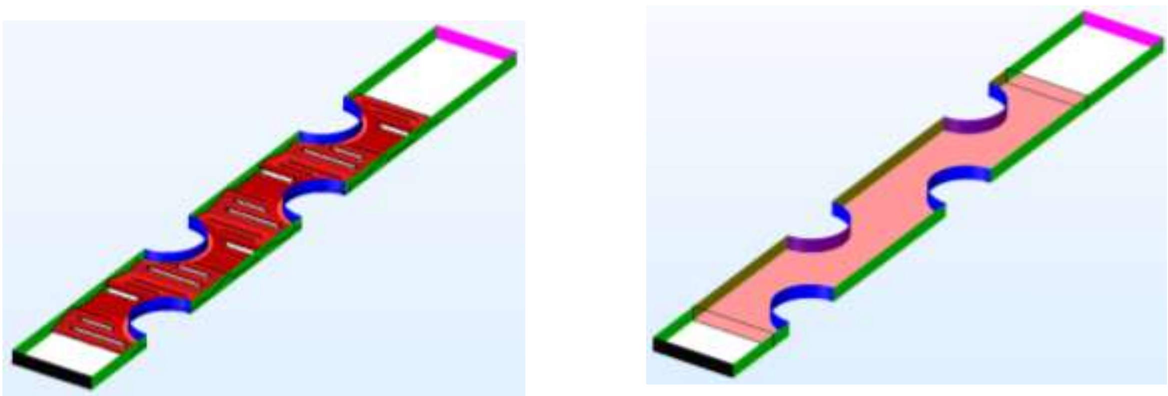

(a) (b)

Fig. 2. Fin simulation: ■ Inlet; ■ Outlet; ■ Tube walls; ■ Symmetry; □ Periodicity-lower (Upper side missing to uncover the model internal structure); ■ Fin wall, only for the detailed model (a); ■ Equivalence model domain, only for the simplified model (b).

Unstructured tetrahedral grid were used for both models, by means of inflation and hexahedral boundary layers on all the wetted surfaces of the model to improve the description of the thermal and fluid boundary layer. Grid sensitivity study was conducted for the detailed fin model. Results for the pressure drop and the overall energy transfer are illustrated in Fig. 3 as a function of the solved degrees of freedom. The flat trend of the overall energy transfer and the small change in the pressure drop justify the selection of the finest tried mesh without need for any further refinement.

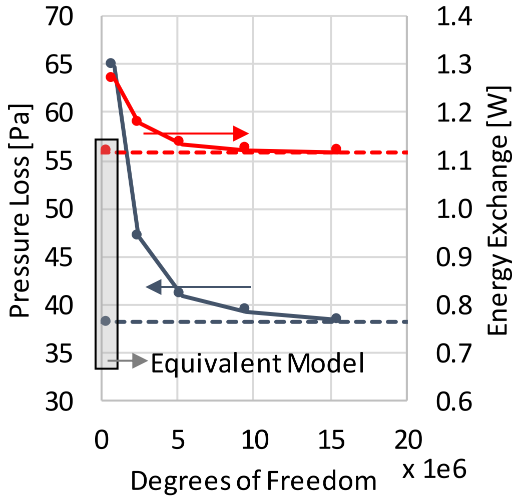

Fig. 3. Grid sensitivity study for the detailed model and comparison with equivalent model.

The results of the detailed fin simulation were then used to choose the best set of parameters for the equivalence model and to assess its accuracy.

The equivalent thermal conduction $\mathbf{k}_s$ was calculated from the fin geometry: the fin material, aluminium, defines the base value for k_s which is used along the y direction: $k_{s\,yy} = k_s$. The louvers significantly decrease the average conductivity of the fin, along the x direction, preventing conduction between rows. Thermal conductivity was then set to $k_{s\,xx} = 0.2k_s$, as the louvers cut approximatively the 80% of the tube pitch. The conduction of the equivalent porous medium along the fin normal direction was set to zero ($k_{s\,zz} = 0$), as out-of-plain conduction is absent in the finned volume, where each fin is not in contact with its neighbours.

The loss coefficients along the main flow direction f_x and the average convective heat transfer coefficient α were obtained as results of a best-fit procedure between the detailed and equivalent model. The normal loss coefficient is assumed high enough to prevent any flow along the tube direction ($\mathrm{f}_z \approx 1000\,\mathrm{f}_x$). The second in-plane coefficient f_y is assumed to be equal to f_x. Despite not formally correct, this assumption allows for simplifying the equivalent model development without a real decrease in the overall accuracy as air flow is expected to have negligible component along the y direction.

The optimized values of $\mathrm{f}_x = 62.5$ m^{-1} and $\alpha = 112.5$ W m^{-2} K^{-1} allowed to fit the global parameter with an approximation of less than 0.4% ,as shown in Fig. 3. The use of the equivalent approach allowed a reduction of more than 30 times the overall number of DOF.

While the integral loss and heat transfer were enforced by best-fitting the equivalent model parameters, therefore can't be used to assess the equivalence model accuracy. Validation between the detailed and the equivalent model can be carried out by comparing local temperatures and partial heat flows. In Fig. 4, the solid temperatures of the two models are compared, i.e. the fin temperature for the detailed model and the equivalent porous medium temperature for the simplified one. Solid temperature differences (Fig. 4c) are always lower than 4°C, with an average error of approximatively 1.5°C, which is satisfactory when compared to the fin temperature span. Heat power distribution between the four rows can be also used for comparison. The percentage of the total heat transfer delivered by each row is reported in Table 2. This comparison demonstrates the good capability of the simplified model to preserve the heat transfer load between the rows.

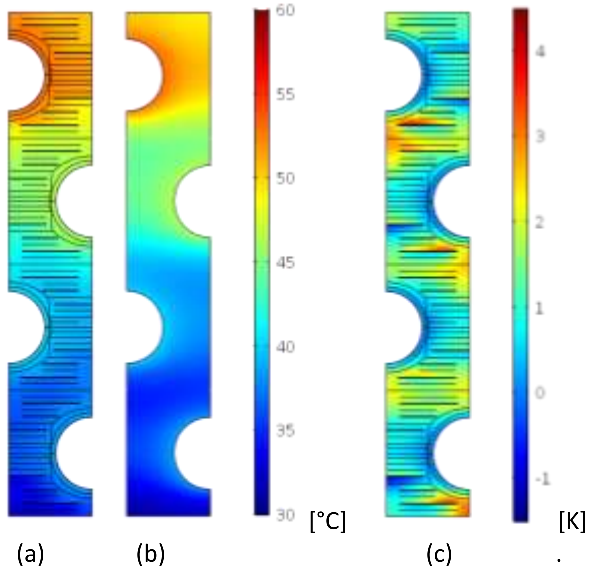

Fig. 4. Solid temperature comparison: (a) detailed model; (b) simplified model; (c) difference detailed minus simplified.

Table 2. Heat transfer distribution between the four rows of the detailed and simplified model.

Row	*Detailed [%]*	*Simplified [%]*
1st	29.4	29.6
2nd	18.8	17.9
3rd	23.9	23.4
4th	27.9	29.1
tot	*100.0*	*100.0*

3.3 Full Model Simulation

The gas cooler simulation couples a 3D model accounting for the air, the tubes and the finned volume, and a 1D model taking care of CO_2 flow inside tubes. The simulation was limited to the upper refrigerant circuit (Fig. 1): section A-A in Fig. 1a is used as a symmetry condition for the air flow domain. The internal temperature of the two tubes crossed by section A-A was set to be equal to the corresponding ones on the upper circuit, assuming a translational periodicity on the refrigerant side of the model. Despite these assumption are contradictory, they allow to half the computational complexity of the problem and can be accepted as reasonable engineering approximation.
Two steel plates 2 mm thick were included into the model to account for conduction effects near the bends of the gas cooler provided by the supporting end plates.
The 3D part of the numerical model is shown in Fig. 5. Table 3 reports the main model materials and boundary conditions, as well as the main coupling operators adopted. The refrigerant side heat transfer coefficient α_{CO_2} was computed using Gnielinski's equation (Gnielinski, 1976), while pressure losses were calculated using the Colebrook-White friction factor.

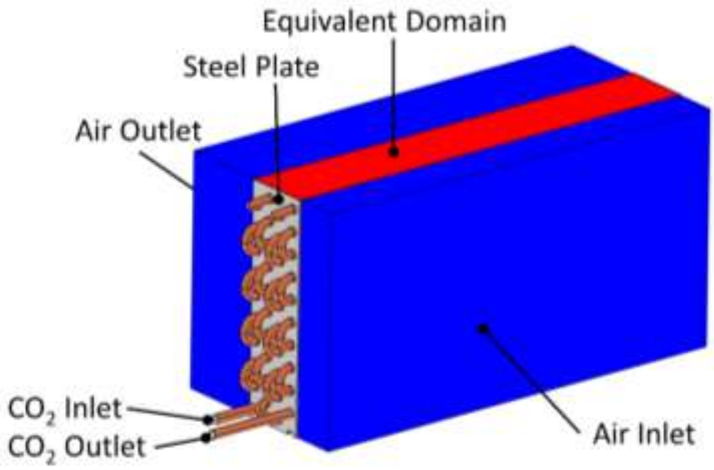

Fig. 5. 3D model domains and materials: ■ Air; ■ Equivalent porous medium domain; ■ Copper; ■ Steel.

The whole model counts 40M degrees of freedom. The simulation was run on a 2 processors Intel Xeon E5-2680 v3 computer with 192 GB RAM.

Table 3. Gas Cooler boundary conditions

Material	**Type**	**Value**
Air	Inlet	Normal velocity $\mathbf{u}$ and Temperature: T_a
Air	Outlet	Relative Pressure: $p = 0$ Pa
Air	External Walls	No slip Condition. Adiabatic Wall
Air	Tubes Walls	No slip Condition. Temperature: $T_a = T_s$
Air	Section A-A	Symmetry
CO_2	Inlet (1D model)	Mass flow $\dot{m}_{CO_2}$ and Temperature: T_r
CO_2	Outlet (1D model)	Pressure
Copper	All uncoupled surfaces	Adiabatic Wall
Steel	All uncoupled surfaces	Adiabatic Wall
Aluminium	All uncoupled surfaces	Adiabatic Wall
Coupling		**Type**
CO_2 ↔ tube internal surface		Heat Flux coupling: $\lvert Q \rvert = \alpha_{CO_2} 2\pi r_i \left(T_{CO_2} - T_s \right)$ [Wm^{-1}]
Equivalent solid ↔ to air flow		Heat Flux coupling : $\lvert Q \rvert = \phi_a \left(T_a - T_s \right)$ [Wm^{-3}]

4 Validation and Results

The numerical results have been validated with experimental results reported in Zilio *et al.* (2007) and Schiochet (2005), obtaining satisfactory match. Results for two operating conditions, reported in Table 4, are summarized in Table 5 in terms of energy balance and average outlet temperature.

Table 4. Validation oprating conditions

	Air Inlet Velocity $\mathbf{u}$	Air Inlet Temperature T_a	CO_2 inlet mass flow $\dot{m}_{CO_2}$	CO_2 inlet pressure p_{CO_2}	CO_2 inlet Temperature T_r
Test 1	1.61±0.01 ms^{-1}	23.0 ±0.05 °C	166.4 ±0.2 kg h^{-1}	9.102 ± 0.002MPa	107.8 ±0.05 °C
Test 2	1.47±0.01 ms^{-1}	17.0 ±0.05 °C	212.8 ±0.2 kg h^{-1}	8.000 ± 0.002MPa	55.9 ±0.05 °C

Table 5. Numerical model validation

	Air Outlet Temp. [°C]	CO_2 Outlet Temp. [°C]	Heat Flow Rate Air Side [kW]	Heat Flow Rate CO_2 Side [kW]
Test 1				
Experimental	45.1±0.05	33.1±0.05	10.8±0.1	10.9±0.06
Numerical	44.0	34.2	10.5	10.6
Test 2				
Experimental	37.0±0.05	32.9±0.05	8.8±0.1	8.5±0.06
Numerical	37.2	32.4	8.9	8.8

In order to check the local accuracy of the model and not only the overall performance, the local temperature on the copper curves for Test 1 were compared between numerical and experimental results. Comparison is shown in Fig. 6, where the experimental measurements (reported from Zilio *et al.* 2007) are compared to the average superficial copper temperature as predicted by the numerical model. The average difference for the first two rows is less than 1 °C, while it increase to an average of 2°C in the third and fourth rows. This precision can be considered satisfactory when compared to the air – CO_2 temperature difference, which can be as high as 60 °C in the 4th row, decreasing to 10 °C in the 1st row.

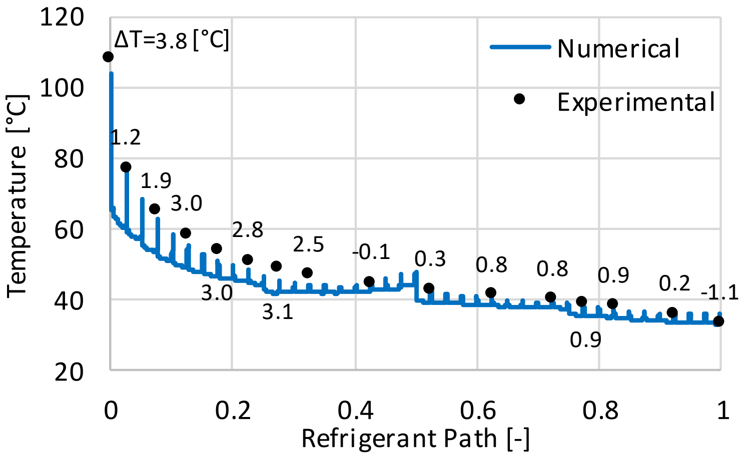

Fig. 6. Numerical model validation: comparison of the copper tube external temperature (difference in °C reported near each experimental point).

The solution of the fluid flow highlighted the uneven temperature distribution of the air through the heat exchanger, caused by the great variation of the CO_2 temperature in the 4th row: the outlet air temperature, 0.1 m downstream the gas cooler outlet, varies from 51 °C to 39°C, as reported in Fig. 7, where the highest temperature corresponds to the CO_2 inlet tube. The map of the heat flux on the fins plane (Fig. 8) explains the cause of this trend. The specific heat flow close to the first tube is almost double than the average, due to the high temperature difference between the fin and the fluid. The heat flux decreases sharply in three tubes, reaching a minimum in the top left corner. This is due to both the presence of the boundary layer, which decreases the air velocity near the top wall, and the low refrigerant temperature (considering the local average between 3rd and 4th row).

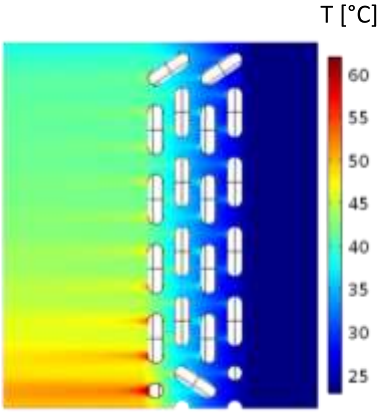

Fig. 7. Air temperature distribution on the symmetry xy plane.

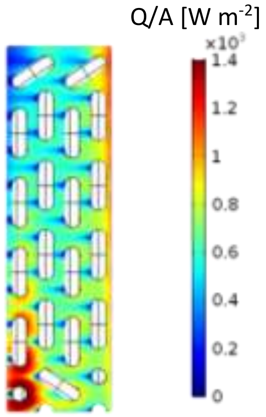

Fig. 8. Specific Heat flow on the symmetry xy plane.

The contemporary solution of both convection and conduction allows to discuss the relative importance of the two phenomena and some collateral effects due to the interaction between the tubes and the side plates. Fig. 9a reports the comparison between the refrigerant temperature and the copper tube average superficial temperature.

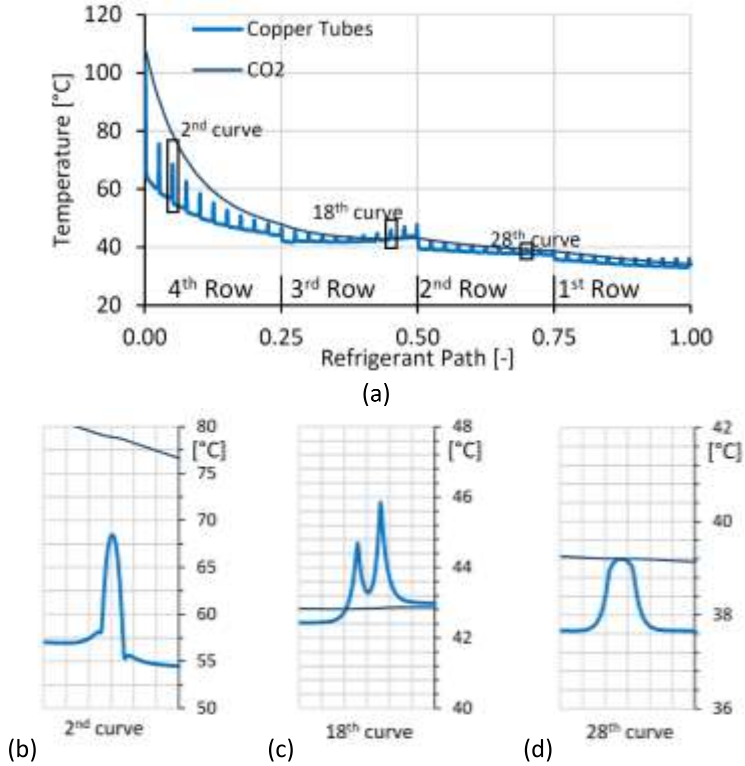

Fig. 9. Average tube temperature and refrigerant temperature along the refrigerant path: (a) complete refrigerant path; (b) detail of the 2nd curve; (c) detail of the 18th curve; (d) detail of the 28th curve.

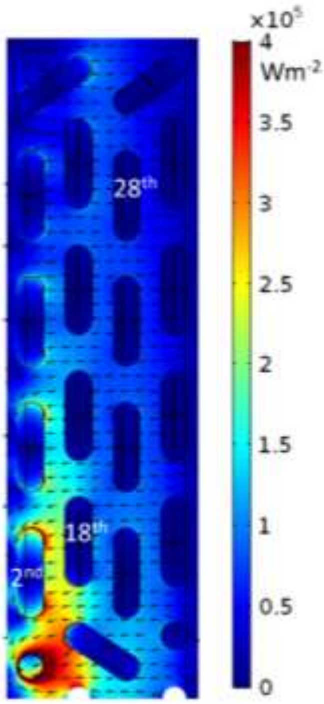

Fig. 10. Heat Flux on the iron side plate.

The wide temperature decrease of the refrigerant inside the gas cooler leads to complex local effects on the curves, as results of the row-to-row conduction on the side plates and the axial conduction of the copper tubes. Three different behaviours are highlighted in Fig. 9b-d.

Fig. 9b reports the temperature trends on the gas cooler second curve. The finned copper tube just before and after this curve is significantly cooler than the refrigerant, as a result of the high temperature difference between the air and the refrigerant. When moving to the curve, the radial heat flow from the refrigerant to the copper and the absence of external convection lead to an increase of the solid temperature. At the same time, the axial conduction towards the finned part of the tube, which is colder, prevents the copper temperature to reach the refrigerant temperature. As result of these effects, the hottest point of the curve is 10°C cooler than the refrigerant, but 10°C hotter than the copper tube just before and after the curve itself. The presence of high temperature gradients in the first tubes lead to high heat fluxes between the first tubes of the fourth row and the last of the third, as visible in Fig. 10. This situation leads to complex and unexpected temperature trend between copper and refrigerant, as for example in the 18th curve, reported in Figure 7c. The copper tube is initially colder than the refrigerant. When approaching the side plates, the tube temperature increases to a maximum: the two spikes on the plot correspond to the two passages across the end steel plate, which is warmer due to conduction from the 2nd curve. The copper tube is then cooled by the refrigerant reaching a minimum temperature slightly greater than the CO_2 temperature. Conduction effects from the 4th to the 3rd row have a global effect visible on the refrigerant temperature, which increases slightly in the last tube of the 3rd row.

Curves and refrigerant reach instead a stable equilibrium at the refrigerant temperature between the end of the first row and the beginning of the second row, as a result of the low temperature gradients between the tubes (Fig. 9d).

All these details are crucial for a correct validation of the numerical model as, for practical reasons, experimental temperatures are measured using probes in contact with the external surface copper tubes and not inside the refrigerant flow. While these temperatures can be close to the refrigerant temperature in some cases (Fig. 7c-d), there might be points affected by strong gradients (Fig. 9c) or locations where the superficial temperature is significantly different from the refrigerant one (Fig. 9b). The numerical model demonstrated to be a useful tool to correctly interpret experimental data.

5 CONCLUSIONS AND FURTHER DEVELOPMENTS

The paper presents a multi physic numerical model of a fin and tube gas cooler using louvered fins. A simplified approach was developed and validated to account for the fins effects, allowing to reduce the computational effort of one order of magnitude in respect of a detailed CFD model describing each single fin. The proposed equivalence model was developed to maintain the flexibility of the CFD models and a multi-physics approach as it contemporary solves the fluid flows (external and internal) and the conduction on the solid domains. The equivalence model was tuned on a single fin simulation: as the only input to this procedure are the geometrical data, as well as the operating conditions, it can be applied independently from any previous knowledge on the fin performance, making this approach suitable for preliminary design of fins and tubes heat exchangers.

The model results are validate against experimental data, both in terms of the overall heat transfer and of the temperature of the curves along the refrigerant path. The model proves to offer good accuracy both in global and local terms.

The model demonstrates the capability of quantifying the effects of conduction due to the fins and the supporting end-plates of the gas cooler. It can show as copper curves surface temperature is affected by row to row conduction and tube axial conduction. As a result of these effects, the curves surface temperature can differs significantly from the refrigerant one. Thanks to this feature, the model can be used to critically

evaluate experimental temperature measurements and the expected difference between the measured values and the refrigerant temperature, when measures are acquired by means of contact probes.
While uniform air conditions are used in this case, in order to reproduce the experimental conditions, the numerical model can handle non uniform air-flow condition, allowing to discuss real applications.
In particular, two main fields of application are identified: the first one is related to the actual position of the fan with respect to the finned coil or the position of the heat exchanger and fan case with respect to the wall or any impediment affecting the fan performance. The above mentioned design or installation issues impact on air side heat transfer coefficient and temperature distribution. The second field of investigation relates to the effects of the fan speed regulation at variable operating conditions; it is actually common practice to modulate fan speed, especially when a low load occurs or outdoor air temperature is old. This topic is intrinsically connected to the heat exchanger design and performance, as well as to the high pressure optimisation, as described in Cecchinato *et al.* (2010) and Cecchinato *et al.* (2012), being the refrigerant temperature out of the gas cooler strongly affected not only by the air temperature but also by its mass flow rate.

NOMENCLATURE

Capital		
A	*area*	(m^2)
Cp	*heat capacity at constant pressure*	$(J\ kg^{-1}K^{-1})$
$\mathbf{F}_L$	*loss force*	$(N\ m^{-3})$
Q	*heat flow*	(W)
T	*temperature*	(K)
V	*volume*	(m^3)
Lower-case		
b	*fin pitch*	(m)
$\mathbf{f}$	*friction factor*	(m^{-1})
i	*intermittency*	$(-)$
k	*thermal conductivity*	$(W\ m^{-1}K^{-1})$
$\dot{m}$	*mass flow*	$(kg\ s^{-1})$
p	*pressure*	(Pa)
r_i	*tube internal radius*	(m)
$\hat{\mathbf{t}} = \mathbf{u}/\lvert\mathbf{u}\rvert$	*unit vector*	$(-)$
$\mathbf{u}$	*velocity vector*	$(m\ s^{-1})$
u, v, w	*velocity components*	
x,y,z	*reference system*	(m)

Greek		
α	*surface convective heat transfer coefficient*	$(W\ m^{-2}K^{-1})$
α_v	*volumetric convective heat transfer coefficient*	$(W\ m^{-3}K^{-1})$
θ_p	*solid volume fraction*	$(-)$
ρ	*density*	(kgm^{-3})
Subscripts		
CO_2	*carbon dioxide*	
L	*loss*	
a	*air*	
r	*refrigerant*	
s	*solid*	

REFERENCES

Aslam Bhutta M M, Hayat N, Bashir M H, Khan A R, Ahmad K N, and Khan S. 2012. CFD applications in various heat exchangers design: A review. Applied Thermal Engineering, 32: 1-12.

Bensafi A, Borg S, Parent D. 1997. CYRANO: a computational model for the detailed design of plate-fin-and-tube heat exchangers using pure and mixed refrigerants, International Journal of Refrigeration, 20(3): 218–228.

Cecchinato L, Corradi M, Cosi G, Minetto S, Rampazzo M, 2012. A real-time algorithm for the determination of R744 systems optimal high pressure , International Journal of Refrigeration 35: 817-826

Cecchinato L, Corradi M, Minetto S, 2010. A critical approach to the determination of optimal heat rejection pressure in transcritical systems, Applied Thermal Engineering 30: 1812-1823

Comsol Multiphysics 5.3 www.comsol.com [last retrieved: 20/11/17]

Dezan D J, Salviano L O, Yanagihara J I. 2016. Heat transfer enhancement and optimization of flat-tube multilouvered fin compact heat exchangers with delta-winglet vortex generators, Applied Thermal Engineering, 101:576-591

Ge Y T, Cropper R T. 2009. Simulation and performance evaluation of finned-tube CO2 gas coolers for refrigeration system, Applied Thermal Engineering, 29: 957–965

Gnielinski V. 1976. New equations for heat and mass transfer in turbulent pipe and channel flow, International Chemical Engineering, 16(2):359–67

Gupta D K, and Dasgupta M S. 2014. Simulation and performance Optimization of finned-tube gas cooler for trans-critical CO2 refrigeration system in Indian context; International Journal of Refrigeration 38: 153-167.

Koern M R, Brix W, Elmegaard B and Larsen L F S. 2011. Performance of residential air-conditioning systems with flow maldistribution in fin-and-tube evaporators. International journal of refrigeration, 34(3): 696-706.

Koern M R, Elmegaard B and Larsen L F S. 2013. Comparison of fin-and-tube interlaced and face split evaporators with flow maldistribution and compensation. International journal of refrigeration, 36(1): 203-214.

Lanping Z, Xitao G, Lei G and Zhigang Y. 2017. Numerical study on airside thermal-hydraulic performance of rectangular finned elliptical tube heat exchanger with large row number in turbulent flow regime, International Journal of Heat and Mass Transfer, 114: 1314-1330.

Mao J N, Chen H X, Jia H, Wang Y Z and Hu H M. 2013. Effect of air-side flow maldistribution on thermal–hydraulic performance of the multi-louvered fin and tube heat exchanger. International Journal of Thermal Sciences, 73: 46-57.

Menter F R, Langtry R B, Likki, S R, Suzen, Y B, Huang, P G and Volker, S. 2004. A correlation-based transition model using local variables: Part I—model formulation, ASME Turbo Expo 2004: Power for Land, Sea, and Air, 57-67. American Society of Mechanical Engineers.

Moukalled F., Verma S., and Darwish and M. 2011. The use of CFD for predicting and optimizing the performance of air conditioning equipment. International Journal of Heat and Mass Transfer, 54(1): 549-563.

Rossetti A, Minetto S and Marinetti S. 2015a. A simplified thermal CFD approach to fins and tube heat exchanger: Application to maldistributed airflow on an open display cabinet, International Journal of Refrigeration 57: 208-215.

Rossetti A, Minetto S and Marinetti S. 2015b. Numerical modelling and validation of the air flow maldistribution in the cooling duct of a horizontal display cabinet, Applied Thermal Engineering, 87: 24-33

Santosa ID M C, Gowreesunker B L, Tassou S A, Tsamos K M, GE Y, 2017. Investigations into air and refrigerant side heat transfer coefficients of finned-tube CO_2 gas coolers, International Journal of Heat and Mass Transfer 107: 168–180

Schiochet G. 2005. Analisi numerica e sperimentale del processo di raffreddamento di anidride carbonica supercritica in uno scambiatore a batteria alettata. Master Thesis, University of Padova (Italy)

Shina A, Chattopadhyay H, Iyengar A K, Biswas G. 2016. Enhancement of heat transfer in a fin-tube heat exchanger using rectangular winglet type vortex generators, International Journal of Heat and Mass Transfer, 101: 667-681.

Singh V, Abdelaziz O, Aute V, and Radermacher R. 2011. Simulation of air-to-refrigerant fin-and-tube heat exchanger with CFD-based air propagation. International Journal of Refrigeration, 34(8): 1883-1897

Singh V, Aute V, Radermacher R, 2010. Investigation of effect of cut fins on carbon dioxide gas cooler performance, HVAC&R Research 16 (4)

Soo Lee M, Li Z, Ling J and Aute V. 2017. A CFD Assisted Segmented Control Volume Based Heat Exchanger Model for Simulation of Air-to-Refrigerant Heat Exchanger with Air Flow Mal-distribution. Applied Thermal Engineering. 131: 230-243. 10.1016/j.applthermaleng.2017.11.094.

Zilio C, Cecchinato L, Corradi M and Schiochet G. 2007. An Assessment of Heat Transfer through Fins in a Fin-and-Tube Gas Cooler for Transcritical Carbon Dioxide Cycles, HVAC&R Research 13(3): 457-469.